ISSN 1063-7737, Astronomy Letters, 2015, Vol. 41, No. 11, pp. 613–632. © Pleiades Publishing, Inc., 2015.
Original Russian Text © V.P. Arkhipova, O.G. Taranova, N.P. Ikonnikova, V.F. Esipov, G.V. Komissarova, V.I. Shenavrin, 2015, published in Pis'ma v Astronomicheskiĭ Zhurnal, 2015, Vol. 41, No. 11, pp. 665–685.

Symbiotic Nova V1016 Cygni: Evolution of the Dust Envelope and the Gaseous Nebula

V. P. Arkhipova*, O. G. Taranova, N. P. Ikonnikova, V. F. Esipov, G. V. Komissarova, and V. I. Shenavrin**

Sternberg Astronomical Institute, Moscow State University, Universitetskii pr. 13, Moscow, 119991 Russia

Received June 16, 2015

Abstract—As a result of the next cycle of our long-term monitoring, we present our $UBVJHKLM$ photometry for the symbiotic nova V1016 Cyg in 2008–2014. The star continued to systematically fade and redden in UBV: over this period, the brightness declined by $0^m.1$ in V and by $0^m.2$ in B and U, the $B-V$ color index increased by $0^m.1$, and $U-B$ barely changed. On the color–color ($U-B$, $B-V$) diagram, the star moved approximately horizontally rightward with a slight bluing in $U-B$ starting from 2000. Our $JHKLM$ photometry has shown a decline in the mean infrared (IR) brightness and a rise in the mean IR color indices after 2004 due to an increase in the optical depth of the dust envelope. The brightness decline and reddening of the Mira in the near infrared reached their extreme values over the entire period of the system's observations by the end of 2014. The pulsation period of the Mira is determined with confidence: $P = 465 \pm 5$ days. The distance to the Mira, $D = 2.92 \pm 0.16$ kpc, and its parameters, the radius $R_* = (470 \pm 50)\ R_\odot$ and luminosity $L_* = (9200 \pm 1900)\ L_\odot$, have been estimated from the observations of V1016 Cyg at its maximum J brightness and at its minimum $J-H$ color index. The temperature of the star during its pulsations varied within the range $T_* = 2100$–2700 K. We have estimated the parameters of the dust envelope near its maximum (in 2004) and minimum (in 2012–2014) IR brightness. The mass of the dust envelope almost doubled in ten years, with the rate of dust supply being $\Delta M_d \sim 10^{-7}\ M_\odot\ \mathrm{yr}^{-1}$. Using a low-resolution spectrograph, we performed absolute spectrophotometry for V1016 Cyg in 1995–2013 in the range λ4340–7130 Å. We have shown that almost all absolute fluxes in lines and in continuum at λ4400 Å decrease monotonically after 2000, while the relative intensities of [O III], [Fe VII], and [Ca VII] lines increase after the minimum that probably occurred in the 1990s. The significant (approximately by a factor of 10 from 1995 to 2013) decrease of the flux in the Raman O VI λ6825 line reflects a change of conditions in the formation zone of this line due to the absorption of some O VI λ1032 photons in the newly forming dust envelope of the cool component.

DOI: 10.1134/S1063773715110018

Keywords: *symbiotic stars, UBV observations, infrared observations, fluxes in emission lines, nebular continuum, post-outburst spectroscopic evolution, V1016 Cyg.*

INTRODUCTION

Symbiotic stars are separated by their properties into two classes: classical symbiotic stars, which are in the majority, and symbiotic novae, about ten of which are known. The difference between these classes lies in such observed properties as the outburst amplitude, the recurrence of outbursts, the presence of a dust envelope, and the variability of the cool component in the binary star system. The orbital periods of the stars apparently differ significantly, although the absence of a sharp boundary in the distribution of periods, as the recent discovery of a "strange" symbiotic nova in Sagittarius shows (Hümmerich et al. 2015), cannot be ruled out either.

Symbiotic novae still remain an inadequately studied class of variable binary stars due to the serendipity of their discovery, their small number, and significant gaps in the history of their evolution during and after outbursts. It is possible to establish the pre-outburst behavior and the rise in brightness based on patrol plates from a number of observatories worldwide, though with large gaps. In the second half of the 20th century, the best photometric and spectroscopic data were obtained for two bright (in outburst) symbiotic novae, V1016 Cyg and HM Sge, which are very similar in their properties.

*E-mail: vera@sai.msu.ru
**E-mail: ikonnikova@gmail.com

A nova-like outburst of V1016 Cyg with an amplitude of about 4^m occurred in 1964 and was detected only in 1965 (McCuskey 1965). After its discovery, the star was intensively studied in various spectral ranges by many authors; the references to their papers predominantly before 1990 can be found in our previous paper (Arkhipova et al. 2008). A fairly complete overview of the results of the investigation of V1016 Cyg has been presented recently by Hinkle et al. (2013).

Despite numerous estimates, the orbital period of V1016 Cyg still remains unknown.

Based on their observations of the variability of hydrogen and Fe II lines, Taranova and Yudin (1983) suggested that the period should be more than 20 years. Munari (1988) found from his analysis of infrared (IR) observations that the ejections of dust were repeated with a period of 6 years and associated this with the orbital period. Based on the measured radial velocities of narrow Fe II lines in 1978–1985, Wallerstein (1988) showed that the orbital period of the system is more than 25 years or the orbit is significantly elliptical.

Nussbaumer and Schmid (1988) estimated the orbital period from the ultraviolet flux variations in O I and Mg II lines to be 9.5 years.

Based on their optical and IR photometry and ultraviolet spectroscopic data, Parimucha et al. (2000, 2002) detected a period of 15 years. They suggested a triple system in which the unresolved pair of stars containing a hot component has this period, while the distant red giant, a Mira, undergoes an enhanced mass loss as it passes through its periastron. However, our subsequent photometric observations did not confirm this period in the optical and IR bands.

Schild and Schmid (1996) found the period from their polarization observations of the O VI λ6825 Å line in 1991–1994 to be within 80 ± 25 years and estimated the linear separation between the components, 23 ± 5 AU, by assuming a total binary mass of 2 $M_\odot$ and a distance of 2 kpc. Having continued their observations in 1997–1998 (Schmid and Schild 2002), they concluded that the orbital period of V1016 Cyg should be longer, ~150–200 years, and that the binary system in these years was in conjunction. Taking the distance to the star to be 3.4 kpc (Whitelock et al. 1987) and the total binary mass to be 2 $M_\odot$, they estimated the angular separation between the components to be 10–15 mas. They pointed out that polarization observations allow the orbital period to be obtained in principle when these observations would cover a larger part of the binary orbit.

Brocksopp et al. (2002) obtained images of the nebula surrounding the star in emission lines and in continuum with the Hubble Space Telescope in November 1999. Provided that the image centers at λ2180 and 5470 Å belong to the hot and cool components, respectively, they measured the angular separation between the binary components, 42.4 mas, and taking the distance to the star to be 2 kpc and the total binary mass to be 2 $M_\odot$, they estimated that the minimum orbital period should be 544 years and the separation between the components in 1999 was 84 AU.

Thus, the question about the orbital period of V1016 Cyg remains unsolved.

In our previous paper (Arkhipova et al. 2008), we analyzed the photometric observations of the star from 1971 to 2007 performed with a UBV photoelectric photometer attached to a Zeiss-600 telescope at the Crimean Station of the Sternberg Astronomical Institute, the Moscow State University. Significantly, the photometric system of the telescope has remained unchanged until the present time, which is very important during the observations of objects with strong emission lines in the spectrum, to which all symbiotic stars belong. In this paper, we present the results of our further UBV monitoring of V1016 Cyg obtained over 70 nights in 2008–2014.

The results of our IR photometry for V1016 Cyg in 1978–2008 are presented in Taranova and Yudin (1983, 1986), Taranova and Shenavrin (2000), and Shenavrin et al. (2011). The bolometric absolute magnitude, luminosity, and radius of the Mira and the radius and mass of the dust envelope were determined from our IR photometry. Here, we present our new $JHKLM$ observations of the star in 2008–2014 performed with the same instrumentation, which allowed us to trace the evolution of the dust envelope around V1016 Cyg and to redetermine the parameters of the Mira and the dust envelope from the entire set of IR data over the period 1978–2014.

The spectroscopic observations of V1016 Cyg have been performed repeatedly starting from the papers by Fitzgerald et al. (1966) and O'Dell (1967). In the 1970s and 1980s, the evolution of the optical emission spectrum and the changes in parameters of the star and the envelope after its outburst were investigated by FitzGerald and Pilavaki (1974), Ahern (1975), Mammano and Ciatti (1975), Ciatti et al. (1978), Blair et al. (1983), Oliversen and Anderson (1983), Ipatov and Yudin (1986), Munari (1988), Rudy et al. (1990), Schmid and Schild (1990), and others. The period from 1989 to 1995 turned out to be not covered by optical spectroscopic observations. A spectroscopic monitoring of the star with a 125-cm reflector began at the Crimean Station of the Sternberg Astronomical Institute in 1995. We presented the first results of these observations previously (Arkhipova et al. 2008). In this paper, we present

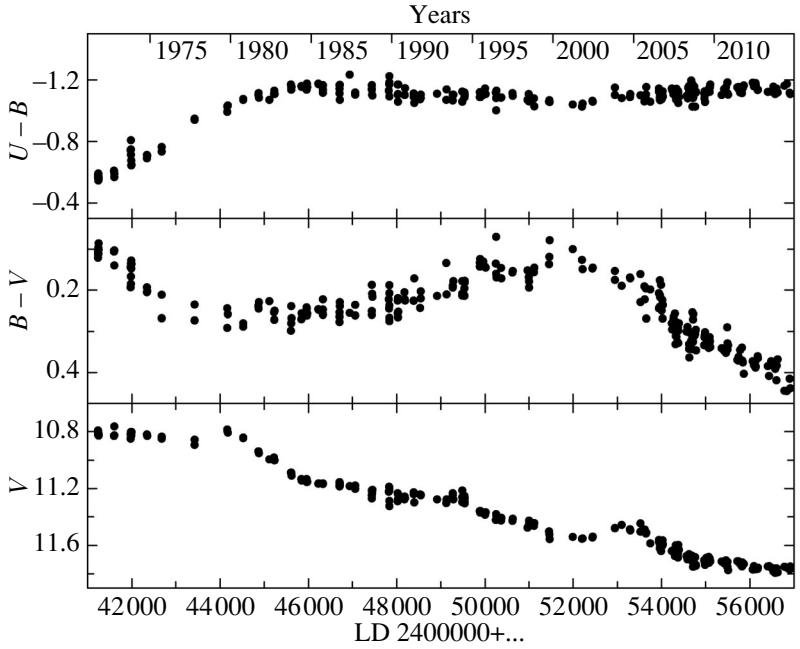

Fig. 1. Light and color curves of V1016 Cyg from all Crimean observations in 1971–2014.

the results of our spectroscopy for V1016 Cyg over the period 1995–2013, along with the reprocessed data from Arkhipova et al. (2008). We determined the absolute intensities of the emission lines in the star whose behavior will be discussed below from the standpoint of the evolution of the emission spectrum after its outburst, the parameters of the gaseous component(=nebula) of V1016 Cyg.

In conclusion, we summarize the results of our long-term study of the evolution of the star after its outburst.

PHOTOELECTRIC UBV PHOTOMETRY FOR V1016 Cyg

Strictly speaking, broadband photometric observations, in particular, in the UBV system, are not very suitable for symbiotic stars because of numerous emission lines in the spectrum. To compare the results of different authors obtained in the "standard" broadband system, the response curves in each band should be known with a good accuracy. Because of slight deviations in the wings of the curves from the standard curve, the various realizations of the UBV system cause noticeable discrepancies between the derived magnitudes if the object has strong emission lines falling into the wings. This is usually removed by comparing the observations obtained simultaneously by different authors and by reducing them to an arbitrarily chosen single system.

Our UBV observations of V1016 Cyg have been performed since 1971 (Arkhipova 1983) with an automated photon-counting UBV photometer at the Cassegrain focus of the Zeiss-600 telescope at the Crimean Station of the Sternberg Astronomical Institute (Lyuty 1971). On the whole, the response curves of the instrumentation reproduce well the standard curves of the UBV bands, except for the red wing of the V band, where the transmission is systematically lower by 5–10% than that in Johnson's V band (Bessell 1990). The magnitudes of the two comparison stars to V1016 Cyg are given in our previous paper (Arkhipova et al. 2008). The errors of the magnitude estimates do not exceed $0\overset{m}{.}02$.

As previously, we took into account the dependence of the V magnitude on the temperature of the thermostatically uncontrolled photometer when reducing our observations. It was checked yearly based on our observations in cold and warm seasons, and it emerged that its variation, within the measurement error limits, was almost constant and equal to about $0\overset{m}{.}007$ per degree. There is no temperature dependence in the B and U bands. All V observations were reduced to $t = +10°$C. The mean error of a single observation did not exceed $\pm 0\overset{m}{.}02$.

The results of our UBV observations in 2008–2014 are presented in Table 1.[1]

Figure 1 shows the V light and $U-B$ and $B-V$ color curves of V1016 Cyg over the entire period of our Crimean observations. Table 2 gives the yearly mean values of V, B, U, $B-V$, and $U-B$ over the

[1] Table 1 is published in electronic form only and is accessible via http://vizier.u-strasbg.fr/cats/J.PAZh.htx.

Table 2. Yearly mean UBV data for V1016 Cyg over the period 1971–2014

Year	JD	V	B	U	$B-V$	$U-B$
1971	2441245	10.812	10.918	10.346	0.106	−0.572
1972	2441600	10.812	10.925	10.331	0.113	−0.594
1973	2441985	10.820	10.974	10.257	0.154	−0.717
1974	2442347	10.823	11.039	10.320	0.216	−0.719
1975	2442680	10.841	11.081	10.333	0.239	−0.748
1977	2443425	10.875	11.128	10.185	0.253	−0.943
1979	2444167	10.795	11.059	10.041	0.264	−1.018
1980	2444525	10.842	11.127	10.053	0.285	−1.074
1981	2444876	10.950	11.172	10.075	0.222	−1.097
1982	2445172	10.994	11.237	10.150	0.243	−1.093
1983	2445613	11.094	11.366	10.214	0.272	−1.152
1984	2445908	11.143	11.401	10.246	0.258	−1.156
1985	2446279	11.164	11.411	10.252	0.249	−1.137
1986	2446711	11.171	11.423	10.292	0.252	−1.131
1987	2447000	11.187	11.439	10.328	0.249	−1.111
1988	2447443	11.234	11.459	10.330	0.225	−1.129
1989	2447830	11.232	11.466	10.302	0.234	−1.164
1990	2448031	11.256	11.494	10.404	0.234	−1.090
1991	2448468	11.249	11.464	10.379	0.215	−1.085
1992	2448540	11.269	11.450	10.318	0.181	−1.132
1993	2449205	11.268	11.445	10.346	0.177	−1.099
1994	2449517	11.265	11.458	10.362	0.193	−1.096
1995	2449950	11.370	11.507	10.396	0.137	−1.111
1996	2450310	11.405	11.552	10.472	0.147	−1.080
1997	2450629	11.420	11.575	10.471	0.155	−1.104
1998	2451048	11.453	11.613	10.549	0.160	−1.064
1999	2451464	11.533	11.636	10.576	0.103	−1.060
2000	2451987	11.540	11.640	10.600	0.100	−1.040
2001	2452203	11.539	11.675	10.662	0.136	−1.013
2002	2452439	11.541	11.687	10.626	0.146	−1.061
2003	2452943	11.478	11.642	10.516	0.164	−1.126
2004	2453226	11.473	11.653	10.564	0.180	−1.089
2005	2453590	11.497	11.696	10.610	0.199	−1.086
2006	2453886	11.588	11.810	10.716	0.222	−1.094
2007	2454314	11.632	11.929	10.823	0.295	−1.107
2008	2454685	11.702	12.013	10.893	0.311	−1.120
2009	2455040	11.706	12.027	10.903	0.321	−1.124
2010	2455460	11.734	12.068	10.928	0.334	−1.140
2011	2455793	11.724	12.091	10.949	0.367	−1.142
2012	2456130	11.761	12.136	10.977	0.375	−1.159
2013	2456551	11.772	12.157	11.026	0.385	−1.131
2014	2456859	11.757	12.192	11.052	0.435	−1.140

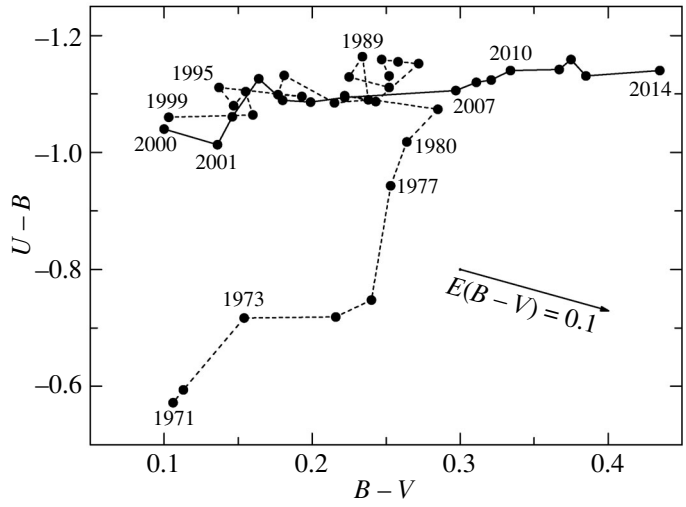

Fig. 2. Motion of V1016 Cyg on the color–color diagram from 1971 to 2014. The yearly mean values are given. The numbers mark the years. The track of the star from 1971 to 1999 and from 2000 to 2014 is indicated by the dashed and solid lines, respectively.

period 1971–2014. Note that the number of observations of the star per year increased noticeably starting from 2005, which allowed brightness fluctuations with an amplitude of about $0^m.1$ to be detected in some observing seasons.

In 2008–2014, the brightness of the star in UBV continued to decline, as before, the $B-V$ color index continued to increase, and $U-B$ decreased insignificantly (became bluer) compared to that in 2000. A noticeable break in the mean light curve, especially in the B band, was observed between 2006 and 2007, whereupon the $B-V$ color index increased by $0^m.07$ in 2008. The reddening of $B-V$ coincided in time with the appearance of a long trend of brightness decline and reddening in the Mira in the infrared.

The color–color ($U-B$, $B-V$) diagram (Fig. 2) shows the yearly mean color indices of V1016 Cyg over the period 1971–2014. Since 1980, the $U-B$ color index, which includes mainly the emission from the hot star and the gaseous component, reached $U-B \sim -1.0$ and has remained at $U-B$ from -1.10 ± 0.05 for the subsequent decades. Given the presence of extinction, this value of $U-B$ points to the existence of an emission Balmer jump, i.e., a continuum of the nebula formed after the nova-like outburst of V1016 Cyg.

The behavior of the $B-V$ color index is nontrivial: it was almost constant in 1983–1990, decreased noticeably by 2000, and has systematically increased by 0.4 from 2000 until now! The emission from all three components of the symbiotic star with a variable contribution of each of them, depending on the time after the outburst, is present in the $B-V$ color index. There is good reason to suggest that the contribution from the hot star in B and V has been small in recent years; the gaseous nebula and the Mira have remained the emission sources.

As we will show below based on our IR observations, the emission from the Mira in V1016 Cyg is significantly distorted by the circumstellar dust envelope. Starting from 1998 and especially after 2004, an increase in the thickness of the dust envelope is observed, while the brightness of the cool star declines, and it becomes redder, which apparently reflected to some extent in the reddening of $B-V$.

The spectroscopic observations of V1016 Cyg presented here showed that the intensities of the [O III] λ5007 and λ4959 lines began to increase with respect to Hβ after 2000. According to our estimates, an increase in the contribution of the nebular lines to the emission from the gaseous envelope in B and V leads to a noticeable increase in the $B-V$ color index. This is also also suggested by the behavior of the $B-V$ color index for some novae once they have entered the nebular phase. V339 Del, for which UBV observations were obtained (Burlak et al. 2015) with the same photometer as for V1016 Cyg, can serve as an example.

Undoubtedly, any variations in absolute emission line intensities are reflected in broadband photometric data. Therefore, studying the line variations is important for analyzing the evolution of the components in V1016 Cyg after its outburst based on UBV data. The contribution of emission lines (Δm) to the photometric UBV bands for V1016 Cyg was first estimated by Skopal (2007) based on the emission line fluxes measured on November 15, 1987, by Schmid and Schild (1990) and UBV data from the catalog of Munari et al. (1992) and from Parimucha

Table 3. $JHKLM$ photometry for V1016 Cyg over the period 2008–2014

JD	J	H	K	L	M	JD	J	H	K	L	M
2454426	7.29	5.84	4.60	2.78	2.22	2455760	8.58	6.97	5.36	3.16	2.50
2454458	7.18	5.75	4.53	2.73	2.18	2455779	8.49	6.85	5.23	3.05	2.30
2454577	7.56	6.15	4.96	3.10	2.48	2455784	8.42	6.79	5.21	3.02	2.40
2454605	7.76	6.32	5.13	3.26	2.60	2455792	8.37	6.72	5.17	3.01	2.37
2454659	8.06	6.64	5.37	3.47	2.88	2455811	8.31	6.71	5.10	2.98	2.33
2454668	8.13	6.66	5.39	3.47	2.86	2455820	8.27	6.66	5.11	2.99	2.42
2454686	8.17	6.72	5.45	3.47	2.75	2455842	8.23	6.64	5.06	2.97	2.27
2454700	8.18	6.75	5.46	3.50	2.88	2455870	8.20	6.58	5.05	2.97	2.27
2454750	8.14	6.72	5.44	3.45	2.80	2455911	8.23	6.68	5.16	3.02	2.24
2454763	8.06	6.65	5.39	3.39	2.72	2456058	9.20	7.59	5.98	3.70	3.00
2454781	7.92	6.54	5.26	3.26	2.56	2456081	9.27	7.66	5.95	3.67	2.96
2454804	7.64	6.30	5.06	3.11	2.48	2456091	9.26	7.64	6.00	3.71	3.00
2454931	7.67	6.14	4.82	2.89	2.23	2456118	9.35	7.70	6.02	3.78	3.00
2454970	7.92	6.31	4.95	2.96	2.29	2456139	9.33	7.69	6.00	3.71	2.94
2454989	8.06	6.48	5.04	3.02	2.36	2456197	8.80	7.15	5.50	3.23	2.51
2455014	8.22	6.62	5.16	3.11	2.55	2456410	8.86	7.18	5.49	3.22	2.54
2455047	8.42	6.81	5.32	3.24	2.55	2456442	9.15	7.44	5.71	3.39	2.64
2455054	8.52	6.89	5.38	3.25	2.57	2456467	9.21	7.60	5.84	3.44	2.83
2455112	8.91	7.21	5.67	3.52	2.88	2456488	9.44	7.70	5.92	3.49	2.75
2455114	8.87	7.20	5.64	3.50	2.90	2456497	9.49	7.77	5.99	3.56	2.83
2455143	9.02	7.38	5.74	3.57	2.90	2456514	9.48	7.85	6.02	3.63	2.92
2455291	8.64	6.92	5.24	3.12	2.45	2456521	9.51	7.84	6.03	3.62	2.93
2455319	8.43	6.68	5.05	2.97	2.32	2456549	9.51	7.92	6.11	3.70	3.15
2455366	8.30	6.54	4.92	2.83	2.16	2456577	9.58	7.96	6.11	3.67	2.92
2455408	8.36	6.58	4.97	2.89	2.35	2456631	9.36	7.66	5.85	3.48	2.78
2455431	8.40	6.66	5.06	2.93	2.22	2456651	9.04	7.34	5.56	3.24	2.62
2455434	8.42	6.70	5.12	2.99	2.28	2456824	8.63	6.87	5.14	2.91	2.26
2455462	8.57	6.87	5.25	3.12	2.50	2456849	8.76	7.01	5.29	3.00	2.27
2455492	8.76	7.11	5.47	3.30	2.48	2456876	9.01	7.24	5.49	3.15	2.42
2455503	8.77	7.17	5.51	3.33	2.64	2456884	8.98	7.27	5.54	3.18	2.43
2455507	8.82	7.16	5.53	3.32	2.65	2456916	9.20	7.48	5.72	3.34	2.69
2455697	9.25	7.66	5.97	3.68	2.90	2456936	9.28	7.56	5.81	3.40	2.67
2455732	8.76	7.18	5.54	3.37	2.60	2456967	9.39	7.72	5.90	3.50	2.71
2455751	8.64	7.04	5.40	3.21	2.40						

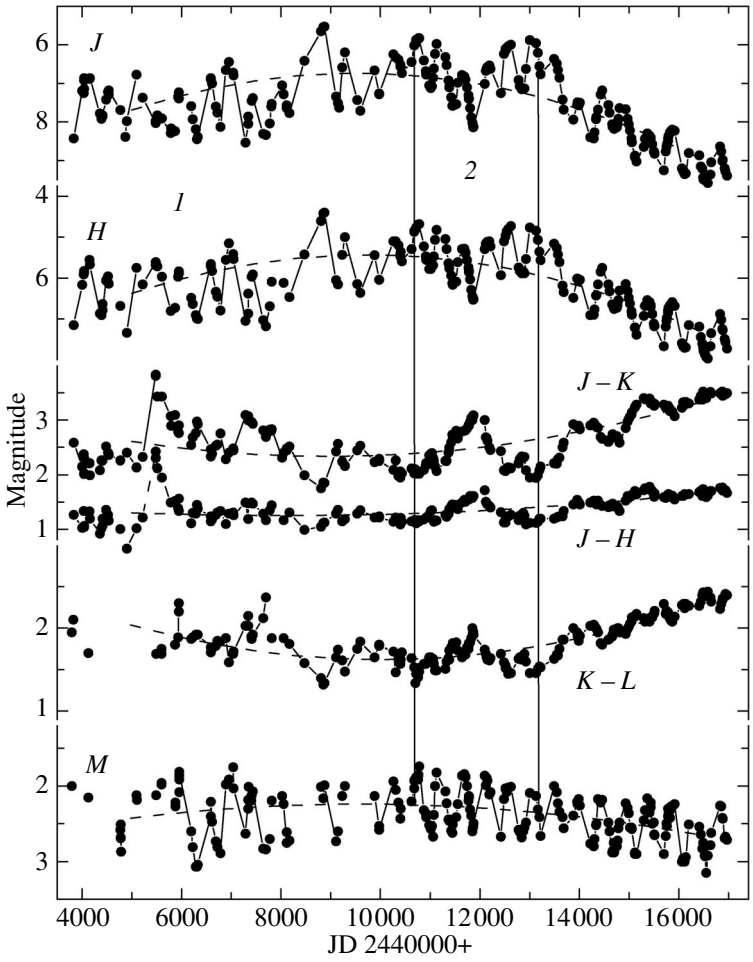

Fig. 3. Observed JHM magnitude and $J-H$ and $J-K$ color variations in 1978–2014. The circles indicate the observations, the dashed lines are the fits to the observed variations by parabolas; for the lines and numbers, see the text.

et al. (2002). Skopal (2007) showed that the correction to the VBU magnitudes for the contribution of emission lines was very significant at that time, $1^m.19$, $1^m.67$, and $1^m.23$, respectively. Once the contribution of lines has been taken into account, the continuum of V1016 Cyg in UBV turned out to be a nebular one with a distinct emission Balmer jump.

Unfortunately, we failed to repeat our estimation of the effect of emission lines in all UBV bands based on our spectroscopic observations after 2000 due to the absence of data on the lines with a wavelength shorter than λ4300 Å. However, the contribution from the lines in V was found to be $\Delta V = 0^m.46 \pm 0.02$ or 35% of the total flux in this band, which is considerably smaller than the estimate by Skopal (2007) from the 1987 data.

INFRARED PHOTOMETRY FOR V1016 Cyg

Our systematic $JHKLM$ photometry (1.25–5 μm) for V1016 Cyg was begun in 1978 and has continued to the present time. All observations have been performed with the 125-cm telescope at the Crimean Station of the Sternberg Astronomical Institute at part of the program of research on circumstellar dust envelopes. The star BS 7796 from the catalog by Johnson et al. (1966) served as a photometric standard. The H, L, and M magnitudes of the standard were estimated from their spectral types based on data from Koornneef (1983). The angular diameter of the exit aperture during the photometry was $\approx 12''$, while the spatial beam separation during chopping was $\approx 30''$ in the east–west direction. The errors of the estimates did not exceed $0^m.03$ in JHK and $0^m.05$ in LM.

The results of our $JHKLM$ photometry for V1016 Cyg in 2008–2014 are presented in Table 3. Figure 3 shows the JHM magnitude and $J-K$ and $K-L$ color variations over the entire period of our observations (1978–2014), the photometric data before 1999 are leftward of the vertical line, the dashed lines indicate the fits to our observations by parabolas. Taranova and Yudin (1983, 1986)

and Taranova and Shenavrin (2000) analyzed the IR photometry for V1016 Cyg before 1999. The $JHKLM$ photometry for V1016 Cyg in 1978–2008 is presented in Shenavrin et al. (2011).

The Observed IR Magnitude and Color Variations of V1016 Cyg

A periodicity is clearly seen in the combined light and color curves (Fig. 3). We performed a Fourier analysis for the entire set of IR photometric data using a computer code from Sperl (1998) improved by Lenz and Breger (2005) and refined the pulsation period of the Mira, $P = 465 \pm 5$ days. Figure 4 shows the observed J and L magnitude as well as $J-H$ and $K-L$ color variations with the pulsation phase of the Mira calculated with the elements $JD_{\min} = 2444003 + 465 \times E$.

Two features can be noted in Fig. 4: the amplitude and scatter of the observed magnitudes in the periodic oscillations decrease with increasing wavelength, while the periodic IR magnitude and color oscillations consist of separate cycles. The open circles and stars indicate the phase dependences for two cycles of observations, respectively: near the minimum (cycle *1*) and maximum (cycle *2*) values of the $J-H$ color index.

The J and H magnitude oscillations in cycle *1* are about $1\overset{m}{.}4$. At the same time, the mean $J-H$ color index remains almost constant, and its value corrected for interstellar extinction with $E(B-V) = 0\overset{m}{.}25$ is $(J-H)_0 = 1\overset{m}{.}04 \pm 0\overset{m}{.}01$, i.e., a value typical for oxygen-rich Miras (Clayton and Feast 1969). Noticeable phase oscillations of the J and H magnitudes at an almost constant $J-H$ color index are possible if the periodic radial pulsations of the Mira are mainly responsible for the phase variations of the IR magnitude and color. For example, the radius of the Mira in cycle *1* can change by almost a factor of 2.

For cycle *2*, the IR magnitude and color variations are similar in pattern to those for cycle *1*, but the presence of a dust envelope is clearly seen: the IR brightness declined, and the Mira reddened.

The mean color index $J-H = 1.71 \pm 0.01$. In the range 1.25–1.65 μm, at a dust-envelope temperature of ~600 K and a Mira temperature of 2000–3000 K, only the emission from the Mira attenuated by the dust envelope is observed, while the fraction of the emission from the envelope itself does not exceed 1–2% (Taranova and Yudin 1983, 1986). Consequently, the $J-H$ color index can serve as an indicator of the optical depth of the dust envelope. In the second cycle, compared to the first one, $\Delta(J-H) \approx 0\overset{m}{.}65$ and then $A(J) \sim 2^m$ if the particles in the dust envelope are similar to dirty silicates (Taranova and Shenavrin 2000).

Apart from the magnitude and color variations of V1016 Cyg with a period of 465 days, two trends are clearly seen (the parabolas in Fig. 3): (1) from the beginning of our observations in 1978 to the end of 1999 and (2) from 2004 to at least the end of 2014, i.e., each trend on a time scale of 10–20 years.

A monotonic rise (decline) in IR brightness occurred with a simultaneous decrease (increase) in IR color indices. The dissipation of the envelope, into which both binary components were embedded before the outburst of the hot source in 1964, continued until the end of 1999; subsequently, the optical depth of the dust envelope began to increase, and this process has continued for the last ten years. Over the entire period of our observations, two "glitches" can be noticed in the periodic IR magnitude variations of V1016 Cyg:

—in the summer of 1983 (marked by number 1 in Fig. 3), when a sporadic ejection of the dust envelope whose parameters were estimated by Taranova and Yudin (1986) occurred in the system;

—in late 1998 and until mid-2001, a decline in IR brightness and a simultaneous increase in IR color indices were observed; subsequently, by 2004, the IR brightness and color almost returned to their 1998 levels. In other words, from 1998 to 2004 (episode 2 in Fig. 3), either the injection (and then dissipation) of dust into the dust envelope or the passage of a dust cloud along the line of sight was observed on a time scale of 2000 days.

Starting from 2004, the mean IR brightness began to decrease, while the color indices began to increase, i.e., the optical depth of the dust envelope increased from 2004 to the end of our observations (November 2014). The brightness decline and reddening of the system in the near infrared reached their extreme values over the entire period of its observations by the end of 2014 (see Table 3 and Fig. 3).

The Distance to the Mira and Its Parameters

To estimate the distance, it is optimal to use the observations when the emission from V1016 Cyg belongs mainly to the Mira, i.e., when the $J-H$ color index and the J magnitude are close to the minimum and maximum ones, respectively.

It can be seen from Fig. 3 that such a combination was observed over 11 nights in the interval JD 245 (0403–0765). The mean J magnitude corrected for extinction (the interstellar one and that in the dust envelope) was $J_0 = (5.94 \pm 0.11)^m$. In this case, the distance to V1016 Cyg will be $D \sim 2.2$ kpc if $M(J) \sim -5.8^m$ for Miras with pulsation periods of 450–612 days (Robertson and Feast 1981).

If we use the period–luminosity relation for Miras from Glass and Feast (1982) in the form $M_{\rm bol} =$

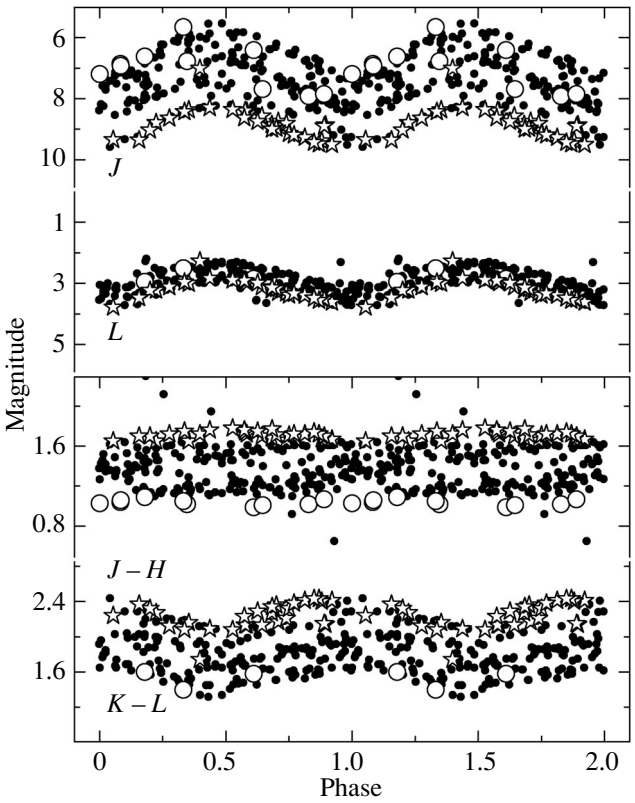

Fig. 4. JL magnitude and $J-H$ and $K-L$ color variations folded with a period of 465 days. The open circles and stars indicate the phase dependences for two cycles of observations, respectively: near the minimum and maximum values of the $J-H$ color index.

$0.76-2.09\log P = -4.80$, where $P = 465$ days, and the mean integrated magnitude of the Mira in the above interval of observations $m_{\rm int} = 7\overset{m}{.}52 \pm 0\overset{m}{.}11$ ($J_0 = 5\overset{m}{.}94 \pm 0\overset{m}{.}11$, $F(J_0) \approx (1.38 \pm 0.13) \times 10^{-15}$ W cm^{-2}, and the integrated flux $F_{\rm int} \approx (2.60 \pm 0.25) \times 10^{-15}$ W cm^{-2}, because the fraction of the blackbody radiation in J with respect to the total emission in the temperature range 2000–3000 K is (0.53 ± 0.02)), then the distance modulus will be $m_{\rm int} - M_{\rm bol} = 5\log D - 5 = (12.33 \pm 0.11)^m$, and the distance to V1016 Cyg will be $D = (2.92 \pm 0.16)$ kpc. The standard error in the distance estimate refers only to the observational errors and disregards the errors in the estimates of the parameters in the relation from Glass and Feast (1982).

The distance to V1016 Cyg was estimated from the period–luminosity relation derived by Whitelock (2009) and Whitelock et al. (2008) for oxygen-rich Miras from the emission of the Mira at 2.2 μm to be $D = (3.10 \pm 0.25)$ kpc. In this case, the uncertainties in the parameters in the period–luminosity relation were also taken into account in the error.

Apart from the distance, we can estimate (1) the parameters of the Mira and (2) the extinction in the dust envelope from the emission of V1016 Cyg in J and H in the above interval of observations. The Mira temperature near the minimum in $J-H$ was $T_* \approx 2600$ K, and the Mira radius is then $R_* = D[F(J_0/B(\lambda,T)]^{0.5} \approx (470 \pm 50)\ R_\odot$, where $F(J_0)$ is the J flux from the Mira, $B(\lambda,T)$ is the flux from a blackbody with a temperature of 2600 K at $\lambda = 1.25$ μm. The luminosity $L_* = 4\pi R_*^2 \sigma T_*^4 = (9200 \pm 1900)\ L_\odot$. The distance was taken to be 2.92 kpc.

On the Parameters of the Dust Envelope around V1016 Cyg

We estimated the parameters of the dust envelope based on the following simplifying assumptions:

—the Mira is embedded in a spherically symmetric and physically thin dust envelope (the source function $B(\lambda) = \varepsilon/\alpha$ does not change);

—the observed magnitude and color variations of V1016 Cyg in the range 1.25–1.65 μm are attributable to the variations in the optical depth of the dust envelope heated by the Mira;

—the temperature of the dust envelope is taken to be 600 K, the dust grains in it are similar to dirty

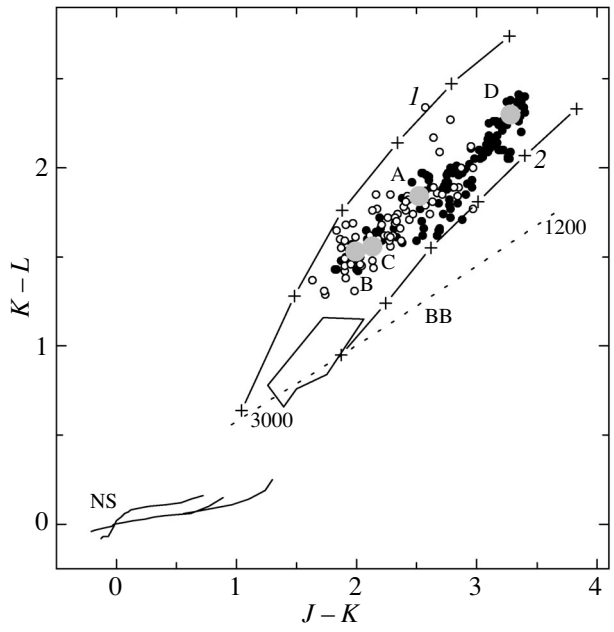

Fig. 5. IR color variations of V1016 Cyg on the color–color $(J{-}K, K{-}L)$ diagram. The open and filled circles indicate the color indices of V1016 Cyg corrected for interstellar extinction with $E(B{-}V) = 0^m.25$ before and after 1999, respectively. The solid lines (NS) indicate the color indices of normal stars of different luminosity classes (Koornneef 1983). The dotted line indicates the color indices of a blackbody (BB) as its temperature changes from 3000 to 1200 K. The region bounded by the solid lines refers to the mean color indices of some of the Miras we observe (Taranova 2000). The solid lines (*1*, *2*) indicate the model color variations of a system consisting of a central star surrounded by a physically thin dust envelope with a constant temperature and a variable optical depth. The large gray circles indicate the mean color indices for four time intervals: A: JD 244 (5932-7341), B: JD 245 (0260-1240), C: JD 245 (2093-3598), and D: JD 245 (6058-6967).

silicates (Taranova and Yudin 1983, 1986; Taranova and Shenavrin 2000), and their radius is 0.1 μm.

In this case, we can use simple relations from Taranova and Shenavrin (2000) and estimate the main parameters of such a system. In our modeling, the photospheric temperature of the Mira was varied within the range 2000–3000 K with a step of 200 K. The parameter β dependent on the type of particles was taken to be 1.35 for dirty silicates (Jones and Merrill 1976). The optical depth of the dust envelope was varied within the range 0–3 with a step of 0.5 at a wavelength of 1.25 μm (J).

Our modeling results are shown on the color–color $(J{-}K, K{-}L)$ diagram (Fig. 5). The calculations were performed at Mira temperatures of 3000 and 2000 K, respectively, and $\tau(J) = 0{-}3$ with a step of 0.5; the dust grain temperature in the envelope is 600 K.

Analysis of Fig. 5 shows the following:

—the observed $J{-}K$ and $K{-}L$ color indices tend to their values typical for Miras while decreasing;

—the bulk of the observed color indices are within the range of Mira temperatures from 2100 to 2700 K and optical depths from 0.5 to 2.5 at a wavelength of 1.25 μm;

—the density of the dust envelope, on average, decreases with increasing Mira temperature.

Using the $J{-}H$ color index as an indicator of the attenuation of the Mira emission by the dust envelope, we can estimate the attenuation in various filters (for particles similar to dirty silicates): $A(J) \approx ((J{-}H)_{\rm obs} - 1.04)/0.3$ in J and $A(V) \approx 3.03A(J)$ in V. Figure 6 shows the attenuations of Mira emission by the dust envelope in J and V. The mean attenuation in V and J was $A(V) = (1.51 \pm 0.22)^m$ and $A(J) = (0.5 \pm 0.1)^m$ from 1978 to 1999 and $(5.8 \pm 0.1)^m$ and $(1.92 \pm 0.04)^m$, respectively, in 2014. The number of averaged values is 73 in the first case and 7 in the second one.

Let us compare the mean parameters of the dust envelope for two intervals: near the 2004 maximum (C: JD 245 (2093–3598)) and over the last period of observations 2012–2014 (D: JD 245 (6058–6967)). The Mira temperature T_* in these intervals was 2500 and 2400 K, the optical depths (at $\lambda = 1.25$ μm) that follow from our model estimates were 1 and 2.25, respectively. In the same intervals, the mean attenuations in J derived from the color excess in $J{-}H$ were $0^m.45$ and $1^m.78$. The noted discrepancies can be explained by the absence of spherical symmetry in the dust envelope. When estimating the dust-envelope

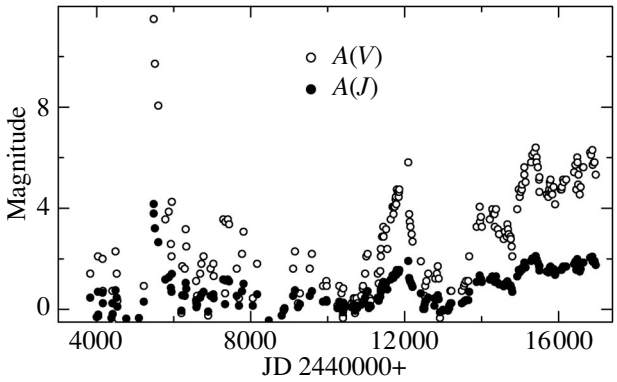

Fig. 6. Attenuation of the Mira by the dust envelope in the system of the symbiotic nova V1016 Cyg in J and V in 1978–2014.

mass, we used our model estimates of the optical depths.

The dust-envelope radius was determined from the relation (McCade 1982): $A = R_d/R_* \approx 0.25(T_*/T_d)^{(4+\beta)/2}$, where the parameter $\beta = 1.35$ if the dust grains are similar to dirty silicates.

The dust-envelope mass was estimated from the relation $M_d \approx 4\pi R_d^2(\rho V_d)(n\Delta R)$, where $\rho \sim 3$ g cm^{-3} is the dust-envelope density, $V_d = 4\pi a^3/3$ is the grain volume, $n\Delta R \approx \tau(\lambda)/Q(\lambda)\pi a^2$, ($Q(\lambda) \sim 0.1$ is the grain absorption efficiency factor at 1.25 μm, $a \sim 0.1$ μm is the grain radius). Then, $M_d \sim 16\pi R_d^2(\rho/3)(a\tau(\lambda)/Q(\lambda)) \approx 5.6 \times 10^{24} A^2 \tau(J)$.

Table 4 summarizes our estimates of the dust-envelope parameters for two intervals.

It follows from the data of Table 4 that the dust-envelope mass almost doubled in ten years, and the rate of dust supply into the dust envelope was $\sim 10^{-7}$ $M_\odot$ yr^{-1}.

SPECTROSCOPIC OBSERVATIONS OF V1016 Cyg

The spectroscopic observations of V1016 Cyg were performed at the Cassegrain focus of the 125-cm reflector at the Crimean Station of the Sternberg Astronomical Institute with a fast spectrograph in the range $\sim\lambda$4000–7500 Å. The slit width was 4″. In 1995–2006, the detector was an SBIG ST-6I 274 × 375-pixel CCD array that with a 600 lines mm^{-1} diffraction grating gave a resolution of ∼5.5 Å per pixel. In 2007–2013, the observations were carried out with an SBIG ST-402 (510 × 765) CCD array with a resolution of ∼2.3 Å per pixel. A log of spectroscopic observations is given in Table 3, where the dates of observations, the spectral range, and the comparison stars are listed. As a rule, the observations were performed with several exposures. The minimum exposure time was chosen in such a way that the strongest lines (Hα and [O III] λ5007) were not overexposed.

The spectra were processed with the standard CCDOPS code and the SPE code (Sergeev and Heisberger 1993). We calibrated the fluxes based on the spectra of standard stars, the data on which were taken from Voloshina et al. (1982), where the absolute energy distributions are given for them in the range λ3225–7625 Å.

Figure 7 presents the spectrum of V1016 Cyg in the range λ4300–7400 Å in absolute energy units

Table 4. Parameters of the Mira and the dust envelope around V1016 Cyg for two epochs of IR observations

Parameters	C: 245 (2480 ± 430)	D: 245 (6300 ± 300)
T_*, K	2500	2400
T_d, K	600	600
R_*, $R_\odot$	470	470
R_d/R_*	22.5	20.2
$R_d/R_\odot$	10600	950
$\tau(J)$	1.0	2.25
M_d, g	1.25×10^{27}	4.5×10^{27}
M_d, $M_\odot$	1.25×10^{-6}	2.25×10^{-6}
ΔM_d, yr^{-1}; $M_\odot$	$\sim 10^{-7}$	

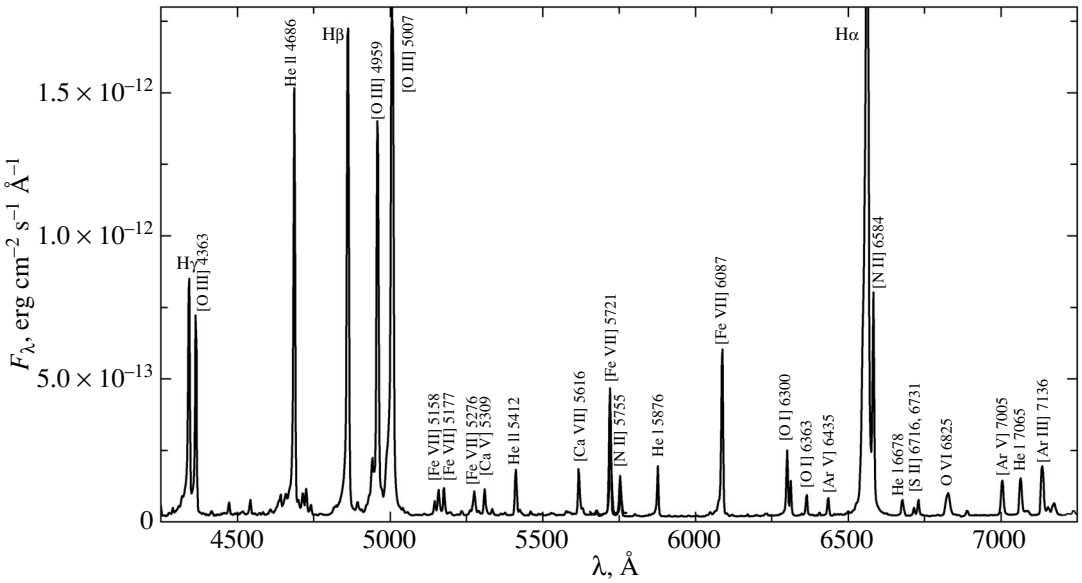

Fig. 7. The spectrum of V1016 Cyg taken on July 31, 2008.

with the identification of emission lines obtained on July 31, 2008.

At present, the optical emission spectrum of V1016 Cyg is represented by numerous emission lines, with the Balmer hydrogen lines, the [O III] λ4363, 4959, 5007 Å lines, the He II λ4686, 5412 Å lines, and the high-excitation [Fe VII] λ5721 and 6087 Å lines being the most intense ones. The weaker emission lines belong to the following species: He I, [O I], [O II], [N II], [S II], [Ar III], [Ar V], [Ca V], and [Fe VI]. The Raman O VI λ6825 line is also present. Such a spectrum is indicative of both a high temperature of the exciting star and a fairly high density of the gaseous envelope.

Table 5. Log of spectroscopic observations for V1016 Cyg

Date	JD	Spectral range	Comparison star
July 29, 1995	2449928	4000–7500	50 Boo
Sep. 27, 1995	2449988	4000–7500	50 Boo
May 30, 2000	2451695	4000–7500	50 Boo
Aug. 29, 2003	2452881	4000–7500	18 Vul
July 17, 2004	2453204	4000–7500	3 Vul
Oct. 4, 2005	2453648	4000–7200	57 Cyg
June 24, 2006	2453911	4000–7500	18 Vul
Aug. 18, 2006	2453966	4000–7500	3 Vul
July 20, 2007	2454302	4000–7200	40 Cyg
Oct. 17, 2007	2454391	4000–7200	40 Cyg
July 31, 2008	2454679	4000–7200	18 Vul
July 23, 2009	2455036	4000–7200	57 Cyg
Aug. 3, 2010	2455412	4000–7200	4 Aql
Sep. 4, 2011	2455809	4000–5600	22 Cyg
Aug. 19, 2012	2456159	4000–7200	40 Cyg
Aug. 21, 2012	2456161	5600–7200	40 Cyg
Aug. 1, 2013	2456506	4000–7500	50 Boo

Absolute Fluxes in Emission Lines and in Continuum from V1016 Cyg over the Period 1995–2013 and Comparison with the Data in 1973–1988

The absolute fluxes in emission lines in the range λ4340–7330 Å and the monochromatic fluxes in continuum at λ4400 Å were the results of our processing of the spectra.

The accuracies of the absolute line and continuum intensities were ~10 and ~30%, respectively. To resolve the blends of Hγ and [O III] λ4363, [O I] λ6300 and [S III] λ6312, [S II] λ6717 and λ6731, we fitted the emission lines by Gaussians. Since the spectral resolution was insufficient, we failed to resolve the [O I] λ6300 and [S III] λ6312 emission lines in the spectrograms before 2007. The [O II] λ7320–7330 doublet was measured as a single whole. In this work, we included the reprocessed 2000–2007 spectra presented previously in Arkhipova et al. (2008).

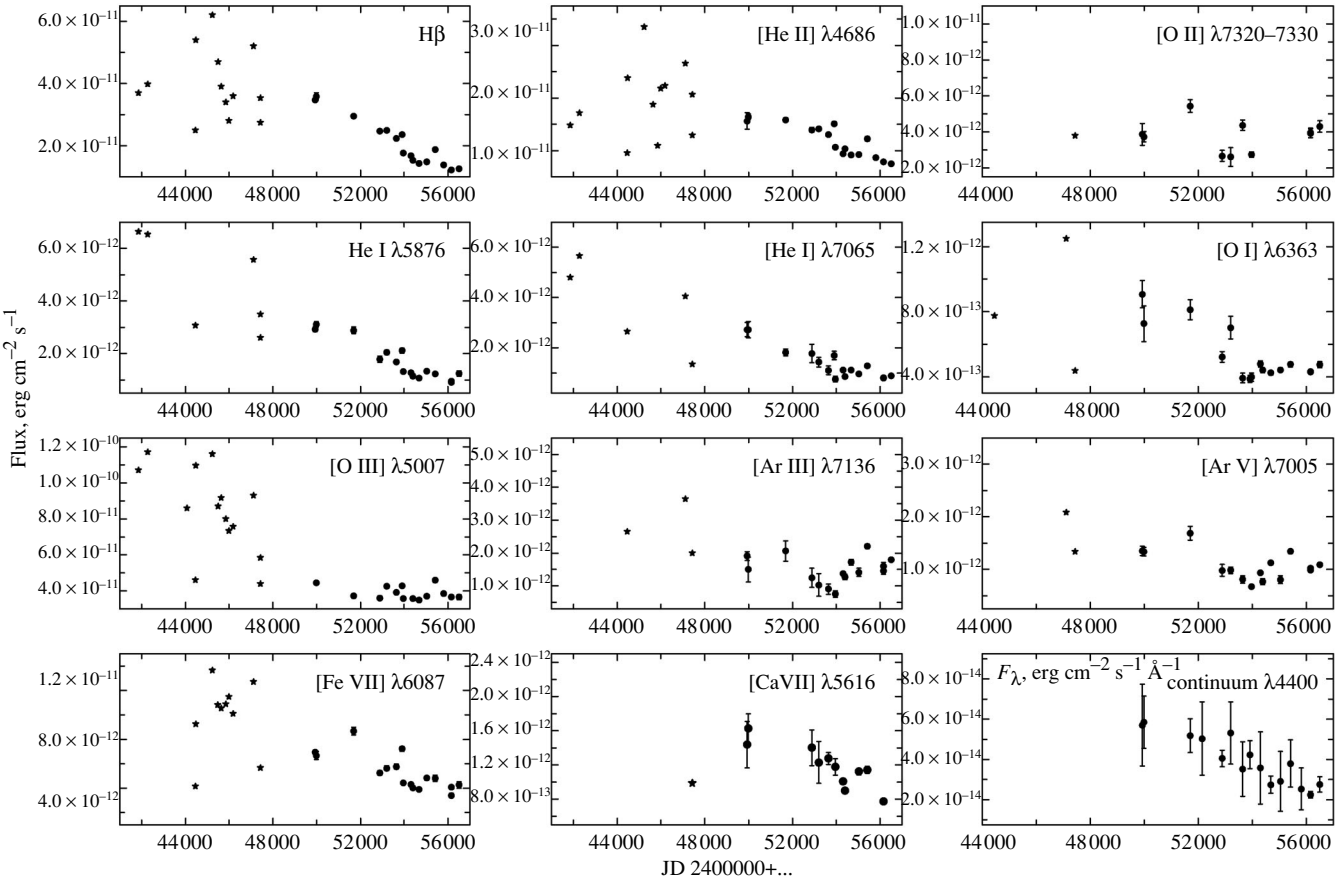

Fig. 8. Variations of the fluxes of emission lines and continuum at λ4400 Å in the spectrum of V1016 Cyg from our data (dots) and published data (stars).

Table 6[2] gives the emission line fluxes in units of 10^{-12} erg cm^{-2} s^{-1}. Figure 8 shows the behavior of the absolute intensities for some lines based on our spectrophotometry in 1995–2013 and the published data from Ahern (1975, 1978), Blair et al. (1983), Oliversen and Anderson (1983), Ipatov and Yudin (1986), Rudy et al. (1990), Schmid and Schild (1990), and Ivison et al. (1991) in 1973–1988.

The Hβ flux changes highly nonmonotonically over the period 1973–1988. Its published measurements gave a spread by more than a factor of 2: from 2.5×10^{-11} to 6.2×10^{-11} erg cm^{-2} s^{-1}. Starting from 1995, our measurements showed a systematic decrease in the flux from 3.6 to 1.3 in units of 10^{-11} erg cm^{-2} s^{-1}. The Hα and Hγ fluxes behaved similarly. The continuum flux at λ4400 decreased proportionally to the Hβ flux.

The fluxes in the He I $\lambda\lambda$5876, 6678, and 7065 lines from 1995 to 2013 changed similarly to those in the Balmer hydrogen emission lines, namely they decreased with time. According to the archival data for 1973–1988, the He II λ4686 flux obtained by different authors with different instrumentation showed a chaotic spread by more than a factor of 3. Our measurements in 1995–2013 suggest a monotonic decrease in the He II λ4686 flux from 1.6×10^{-11} to 0.74×10^{-12} erg cm^{-2} s^{-1}, i.e., by a factor of 2 in 19 years, from 1995 to 2013.

According to the data of different authors from 1973 to 1988, the absolute flux in the nebular [O III] λ4959 and λ5007 lines showed a tendency to decrease at a spread in the data by more than a factor of 2.5. According to our homogeneous observations from 1995 to 2013, the fluxes in the nebular [O III] lines showed no significant trend and remained at $F(\lambda 4959) = (1.25 \pm 0.13) \times 10^{-11}$ erg cm^{-2} s^{-1} and $F(\lambda 5007) = (4.0 \pm 0.4) \times 10^{-11}$ erg cm^{-2} s^{-1}. The auroral [O III] λ4363 line more likely weakened in 1995–2013.

The [Ar V] λ7005 and [Ar III] λ7136 emission

[2] Table 6 is published in electronic form only and is accessible via http://vizier.u-strasbg.fr/cats/J.PAZh.htx.

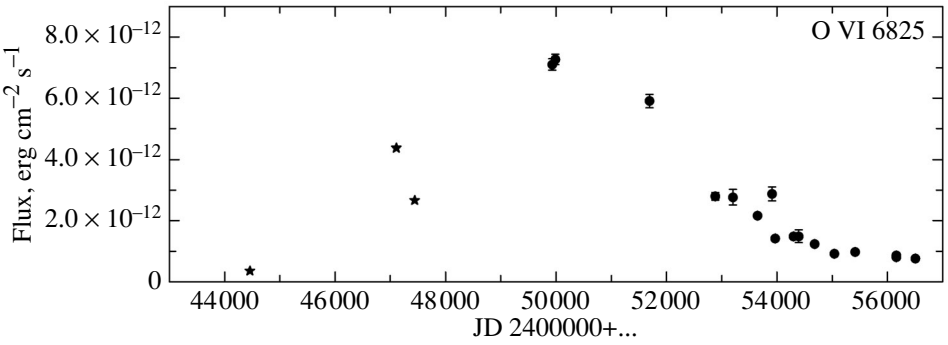

Fig. 9. Variations of the O VI λ6825 line flux. The stars mark the data from Blair et al. (1983), Schmid and Schild (1990), and Rudy et al. (1990). The dots indicate our data.

lines decreased in flux until ~2007 and then began to strengthen.

The highly ionized [Fe VII] λ5721 and λ6087 and [Ca VII] λ5615 lines showed a slight weakening by no more than a factor of 1.5 over the period of our observations. According to Mammano and Ciatti (1975), the [Fe VII] lines began to strengthen in 1971–1974. Ipatov and Yudin (1986) traced the further rise in [Fe VII] flux in 1980–1985. The possible maximum occurred in 1987.

The absolute flux in the [O II] λ7320–7330 doublet underwent no significant changes from 1988 to 2013 and remained at $F = (3.7 \pm 0.7) \times 10^{-12}$ erg cm^{-2} s^{-1} in these years.

Note the time variation of the Raman O VI λ6825 line, the most characteristic feature in the spectra of symbiotic stars. In the 1973–1974 spectrograms from Mammano and Ciatti (1975), it is most likely absent. The first measurement of this line belongs to Blair et al. (1983) and refers to 1980. Its relative intensity in the scale $F(\mathrm{H}\beta) = 100$ was then 1.4. Subsequently, the O VI line flux increased, reaching its peak value near 1995. The line then began to weaken, and by 2013 its intensity decreased by almost a factor of 10 compared to that in 1995. The time variations of the O VI λ6825 line are shown in Fig. 9. We think that the appearance and subsequent strengthening of the Raman O VI line are associated with the growth in the temperature of the hot star and the increase in the number of O VI λ1032 Å photons that reached the H I zone of the wind from the cool component. The decrease in the line intensity after its peak in 1995 is most likely attributable to the change of conditions in the formation zone of this line associated with the absorption of some of the O VI λ1032 photons in the newly forming dust envelope of the cool component.

Thus, according to the observations from 1995 to the present time, most of our measured lines and the continuum at λ4400 Å showed a monotonic decrease in the fluxes to some extent.

Behavior of the Relative Emission Line Intensities from 1965 to 2013

Consider the time variations of the most characteristic line intensity ratios reflecting the change of physical conditions in the gaseous envelope of V1016 Cyg.

The observed relative intensities according to the archival data from O'Dell (1967), Ahern (1975, 1978), Blair et al. (1983), Oliversen and Anderson (1983), Ipatov and Yudin (1986), Rudy et al. (1990), Schmid and Schild (1990), Ivison et al. (1991), and our observations are shown in Fig. 10.

The hydrogen line intensity ratio $F(\mathrm{H}\alpha)/F(\mathrm{H}\beta)$ changed noticeably with time, reflecting the variations of the optical depth in the lines or the influence of impact excitation. From 1974 to 1988, the relative intensity of the Hα line changed within the range 4.0–9.6. The mean value of $F(\mathrm{H}\alpha)/F(\mathrm{H}\beta)$ at the epoch of our observations was 5.4 ± 0.9.

After the nova-like outburst of V1016 Cyg in 1964, the relative intensity of the nebular [O III] λ5007 line grew, reaching its maximum value of $\simeq$3 in 1975. Thereafter, it began to drop, and the ratio $F(\lambda5007)/F(\mathrm{H}\beta)$ decreased by a factor of 2.5 by 1995. Starting from 1995, this quantity shows a systematic increase. By 2013 (in almost 20 years), the relative intensity of the [O III] λ5007 line increased by a factor of 2.5 and is again close to 3.0. The [Ar III] λ7136 line closely follows the behavior of [O III] λ5007 from 1980 to the present time.

The ratio of the auroral O III λ4363 line to the Hγ emission line showed a rapid and significant increase to $F(\lambda4363)/F(\mathrm{H}\gamma) = 1.73$ by 1973–1974 and then a rapid decrease by more than a factor

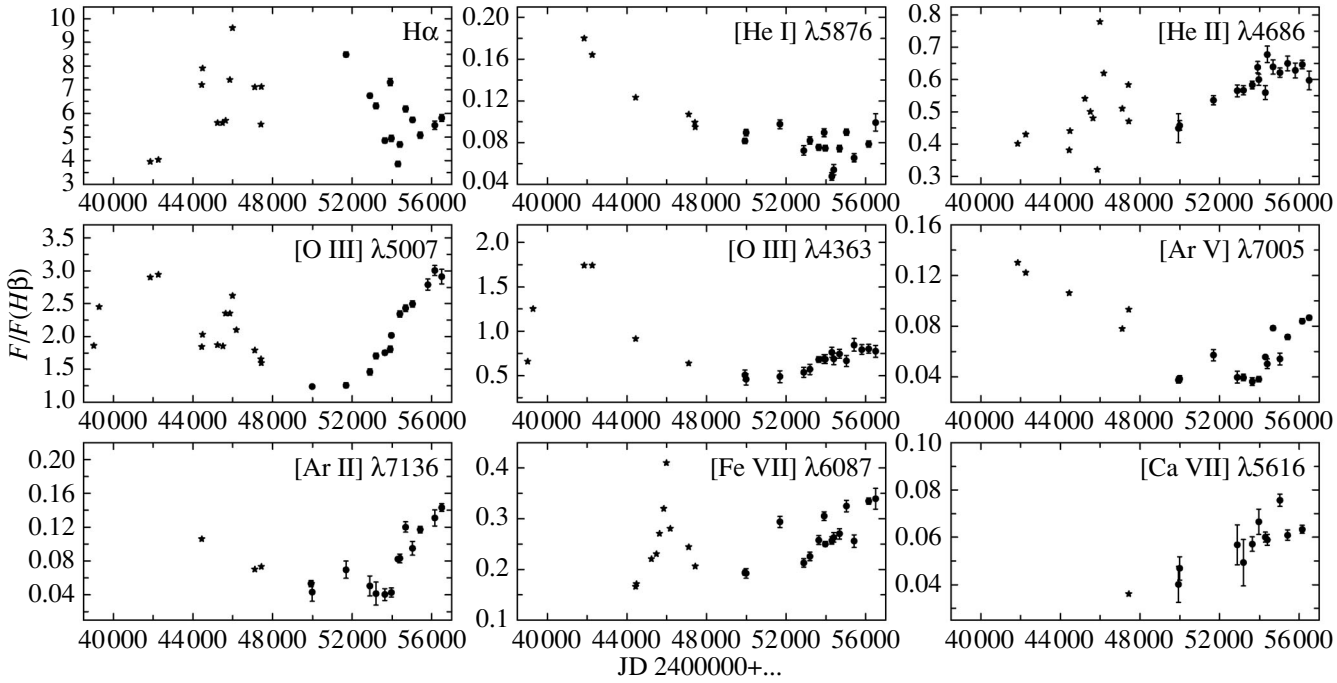

Fig. 10. Time variations of the relative emission line intensities in the spectrum of V1016 Cyg. The stars designate the published data; the dots indicate our observations.

of 3 by 1995. A slow monotonic increase in the ratio $F(\lambda 4363)/F(\mathrm{H}\gamma)$ has been observed in the last 20 years.

The joint behavior of the nebular and auroral [O III] lines can be traced using the $R1 = I(4363)/I(\mathrm{H}\gamma)$, $R2 = I(5007)/I(\mathrm{H}\beta)$ diagram. Based on the 1965–1987 data, such a diagram for V1016 Cyg was first presented by Gutiérrez-Moreno et al. (1995). Our 1995–2013 data supplemented significantly the picture. Figure 11 shows the $R1-R2$ diagram for V1016 Cyg based on the published data and our observations. The motion of V1016 Cyg in the $R1-R2$ plane reflects both a change in the degree of ionization and a change in the nebular's parameters. In the next section, we use this diagram to estimate the parameters N_e and T_e of the nebula.

The ratio of the high-excitation [Fe VII] λ5721 and λ6087 and [Ca VII] λ5716 line intensities to the Hβ intensity shows a systematic increase from 1995 to 2013.

The relative intensities of the He I λ5876 and λ7065 lines systematically decreased after the outburst; their decrease has slowed down in recent years. At the same time, the intensity ratio of He II λ4686 to Hβ increased in 1995–2000, suggesting a rise in the temperature of the ionization source, a hot star. After 2000, the ratio $F(\mathrm{He\,II}\lambda 4686)/F(\mathrm{H}\beta)$ apparently ceased to increase.

Estimation of the Physical Parameters of the Gaseous Envelope (=Nebula) around V1016 Cyg

Ahern (1975, 1978) was the first to estimate the electron density and electron temperature of the gaseous envelope around V1016 Cyg using the intensities of the [Ne III] and [O III] emission lines at λ3869, 4363, and 5007. He obtained the following parameters for epoch 1974: $T_e = 15\,100 \pm 2000$ K and $\log N_e = 6.5 \pm 0.05$ (Ahern 1978).

Using the optical and ultraviolet observations of the star in 1987–1988, Schmid and Schild (1990) determined the parameters of three emission zones in the envelope: for the [O III] zone, they found the electron temperature $T_e = 25\,000$ K and density $\log N_e = 5.8-6.2$. In the low-excitation zone, where the [N II], Si II, and C II lines are emitted, they estimated the temperature to be within the range 10 000–15 000 K; in the [Fe VII] zone, it is above 40 000 K. The parameters were estimated using the diagnostic diagrams.

We attempted to estimate the parameters of the gaseous envelope around V1016 Cyg based on the

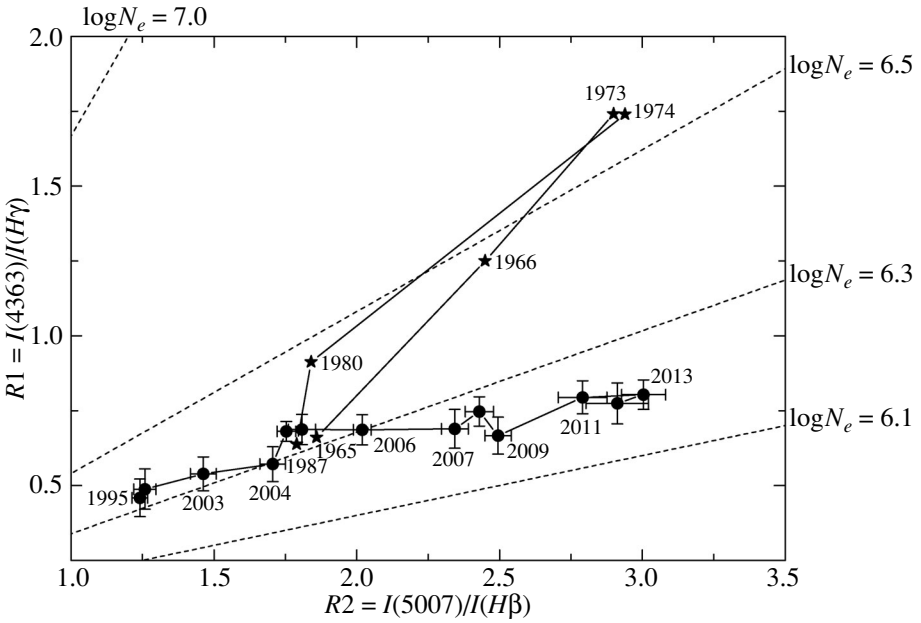

Fig. 11. $R1-R2$ diagram for V1016 Cyg. The stars designate the data from O'Dell (1967) for 1965 and 1967, Ahern (1975, 1978) for 1973 and 1974, Blair et al. (1983) for 1980, and Schmid and Schild (1990) for 1987; the dots indicate our 1995–2013 data. The numbers on the graph denote the years. The dashed lines indicate the lines of constant electron density $\log N_e$ in the range $6.1 \leq \log N_e < 7.0$ at the specified ratios $R1$ and $R2$ from Gutiérrez-Moreno et al. (1995).

2007–2013 spectroscopic data. The spectra that we took previously, before 2007, were not used for this purpose because of their low spectral resolution and the impossibility to resolve the blends of the lines needed for the diagnostics.

To determine the physical parameters of the gaseous envelope around V1016 Cyg, we used the *temden* code from the standard IRAF software package (Shaw and Dufour 1995).

The diagnostic relations should be corrected for extinction. The color excesses $E(B-V)$ for V1016 Cyg derived by different authors differ significantly between themselves and exceed the maximum value of $E(B-V) = 0.24 \pm 0.01$ toward V1016 Cyg from the maps of Schlegel et al. (1998). Apart from the interstellar component, the color excess for V1016 Cyg may also have a variable circumstellar component. For epoch 2007–2013, we estimated the color excess from the Balmer decrement as $E(B-V) = 0.61$ by adopting the interstellar reddening law from Seaton (1979) and the initial Balmer decrement $\mathrm{H}\alpha : \mathrm{H}\beta : \mathrm{H}\gamma = 280.7 : 100 : 47.14$ for $N_e = 10^6$ and $T_e = 10\,000$ K from Brocklehurst (1971). The self-absorption in $\mathrm{H}\alpha$ according to Capriotti (1964) was almost zero, while we estimated $\tau(\mathrm{H}\alpha)$ from the data of Schmid and Schild (1990) for 1987 to be $\sim$15.

A direct measurement of the [N II] λ6548 line led to an unsatisfactory result due to the significant influence of the blue wing of the broad $\mathrm{H}\alpha$ emission line. Therefore, we obtained the intensity of this line using the theoretical ratio $I(6548) = I(6584)/2.96$ (Mendoza 1983).

To estimate the electron density, we used the intensity ratio of the [S II] λ6716/λ6731 doublet, $I(\lambda6716)/I(\lambda6731) = 0.47 \pm 0.02$. It gives a density $N_e = (2-4) \times 10^4$ cm^{-3} at a temperature $T_e = 10\,000-20\,000$ K in the low-excitation zone of the nebula.

The electron temperature of the gaseous envelope was estimated from the intensity ratio of the nebular lines to the auroral one in the [O III] zone, $R(\mathrm{O\ III}) = I(\lambda(4959+5007))/I(\lambda4363) = 8.3 \pm 1.4$, and the [N II] zone, $R(\mathrm{N\ II}) = I(\lambda(6548+6584))/I(\lambda(5755) = 8.0 \pm 1.5$. Note that the ratios of the nebular lines to the auroral one for [O III] and [N II] have increased noticeably in the last decade compared to those 1987–1988.

Knowledge of the electron density is required to estimate the electron temperature in each of the chosen emission zones.

If we take the density obtained above from [S II] for the low-ionization [N II] zone, then the electron temperature from the ratio $R(\mathrm{N\ II})$ turns out to be implausibly high. The density in the [N II] zone

is most likely considerably higher than its estimate from the ratio [S II] λ6717/λ6731, which is near the critical density of the doublet. For example, taking $N_e = (1{-}2) \times 10^5$ cm^{-3} for the low-ionization zone, we will obtain its electron temperature from the ratio of the auroral and nebular [N II] lines, $T_e = 15\,000 \pm 5000$ K. Note that Schmid and Schild (1990) obtained different electron densities for the [S II] and [N II] emission zones in 1987, $\log N_e$[S II] $= 5.35 \pm 0.1$ and $\log N_e$[N II] $= (5.6{-}5.7)$ cm^{-3}, at $T_e = (1{-}3) \times 10^4$ K.

Judging by the $R1{-}R2$ diagram (Fig. 11), the electron density in the [O III] zone from the outburst to the present time changed within the range $\log N_e = 6.2{-}6.5$. In the period of our observations 2007–2013, V1016 Cyg moved over the $R1{-}R2$ diagram rightward, reflecting a slight decrease in $\log N_e$ from 6.3 to ~6.2. For epoch 2007–2013, we adopted the mean value of $\log N_e = 6.25 \pm 0.05$. For R(O III) $= 8.3 \pm 1.4$, the electron temperature in the [O III] zone from our data in this period was then $T_e = 17\,000 \pm 2000$ K.

Comparison of the parameters of the nebular envelope in V1016 Cyg obtained two and four decades after its outburst shows that they changed relatively little (within the limits of their errors): the electron density of the nebula remains high, ~10^6 cm^{-3}, in the [O III] emission zone, as does the electron temperature in this zone, which, though it decreased compared to that in 1987, still remains no lower than 20 000 K. In the [N II] emission zone, the density also remains high (>10^5 cm^{-3}), which may be due to the presence of bipolar outflows in the envelope structure detected by Solf (1983). We think that the moderately significant change in the electron density of the envelope with time is associated with its low expansion velocity, ~50 km s^{-1} (Solf 1983), and with the possible presence of a stellar wind from the hot component.

To estimate the change in the electron density of the gaseous envelope around V1016 Cyg with time, we can also use our data on the hydrogen line fluxes. The flux decreased approximately by a factor of 3 in the last 20 years; this gives a drop in density by a factor of ~1.7.

The monotonic decrease in the hydrogen and He I line fluxes that we observed after 2000 suggests that V1016 Cyg finally enters the true nebular phase of the nova, especially since the relative intensities of the nebular lines began to increase significantly, and the ratio $F(\lambda5007)/F(\mathrm{H}\beta)$ reached 3 by 2013. The rapid growth of this ratio immediately after the outburst peak in the 1960s can be explained by the fact that the envelope was expanding in a less dense circumstellar medium in those years. At present, two parts of the envelope, one facing the cool star and its wind and the other in the opposite direction, are under different ambient density conditions, and the gas parameters in them can differ noticeably.

THE SYMBIOTIC STAR V1016 Cyg HALF A CENTURY AFTER ITS OUTBURST

At present, as a result of all searches for the star's period, it has become clear that the binary system of the symbiotic nova V1016 Cyg is a very wide pair with a large separation between its components. The temperature of the hot component estimated in the early 1990s as 145 000 K (Mürset and Nussbaumer 1994) continued to rise until 2000, which was manifested as an increase in the relative intensity of the He II λ4686 line. There is a gaseous nebula expanding with a velocity of ~60 km s^{-1} in the system (Ikeda and Tamura 2004) whose degree of excitation increases with time. The cool component, a Mira, after the outburst experienced sporadic enhancements of the stellar wind power with the formation of dust due to its pulsational activity (Taranova and Yudin 1983, 1986; Taranova and Shenavrin 2000). After 2000, as we showed in this paper, the dust formation was continuous. Because of their significant separation, the binary components, a Mira with a cold dense wind and a hot subdwarf, possibly, with a fast wind, interacted weakly with one another, evolving independently after the nova-like outburst.

However, the presence of X-ray emission from the star in 1979–1992 (Kwok and Leahy 1984; Mürset et al. 1997) suggests the existence of colliding winds in the binary system. The stellar wind interacting with the cold dense wind from the Mira probably continued to outflow from the hot dwarf after the outburst.

The detection of X rays from V1016 Cyg is quite an established fact. As Mürset et al. (1997) showed, the emission in soft X rays (<1 keV) belongs to a hot star with a temperature of 140 000 K, but in harder X rays, despite the low accuracy of the fluxes, there appears to be emission from a hot gas with a temperature of ~10^7 K. It should be noted that as yet no coronal lines typical for such a gas have been observed during the star's spectroscopic observations.

Our broadband photometric UBV observations since 1971 showed that the fading of the star after its outburst was only about $1^m.0$ by 2014. Since 2000, the yearly mean V brightness declined by only $0^m.25$, while the $B{-}V$ color index increased by $0^m.4$ and the $U{-}B$ color became bluer by $0^m.1$. We are inclined to associate the significant growth of the reddening of $B{-}V$ with the growth of the dust component of the Mira under the assumption that the part of the nebular envelope expanding toward the Mira fell into

the zone of the dust envelope around the Mira. However, $U-B$ does not reflect the growth of extinction at all. In our opinion, the systematic reddening of the Mira after 2004 and the change in the effect of bright lines in B and V are responsible for the growth of the reddening of $B-V$. In particular, the latter is attributable to the increase in the relative intensities of the nebular [O III] lines falling into the B and V passband wings.

If the expansion velocity of the nebular envelope around V1016 Cyg is taken to be $V_{\rm exp} = 60$ km s^{-1} (Ikeda and Tamura 2004), then by 2000 the envelope radius must have been $R_{\rm neb} = 440-660$ AU or $\sim 0\farcs2-0\farcs3$ at a distance $D = 2-3$ kpc. The angular radius of the envelope with these parameters turns out to be significantly larger than the separation between the components $\Delta\theta = 0\farcs042$ measured by Brocksoppet al. (2002), i.e., in 2000 the nebula was far beyond the binary orbit, and the growth of the dust envelope around the Mira after 2000 could not affect strongly the reddening of the nebula if it has a spherical shape.

CONCLUSIONS

We presented the results of our long-term series of $UBVJHKLM$ photometry and absolute spectrophotometry for the symbiotic nova V1016 Cyg.

Analysis of the UBV data, including our long-term observations started in 1971, showed that the brightness of V1016 Cyg continued to decline at a mean rate of about $0\fm03$ per year. The mean magnitudes of the star in 2014 became $V = 11\fm76$, $B = 12\fm19$, and $U = 11\fm05$. The brightness fluctuations in all bands around the yearly mean value did not exceed $0\fm05$ over the entire history of observations.

The color indices underwent significant changes over the entire period of observations 1971–2014. The $U-B$ color index became bluer before 1980 and reached -1.07 in 2000, whereupon it remains at $U-B = -1.10 \pm 0.05$ with slight fluctuations. The $B-V$ color index increased by $0\fm2$ from 1971 to 1980 and became $+0\fm3$ and then again returned to $+0\fm1$ by 2000. A systematic increase in $B-V$ was observed after 2000, and it became $+0\fm43$ in 2014. Such a reddening of $B-V$ cannot be attributed only to an increase in the circumstellar extinction associated with the formation of a new dust envelope around the red component. We think that the reddening of $B-V$ is associated both with the Mira reddening after 2000 and with the change in the effect of emission lines in B and V due to an increase in the relative intensity of the [O III] λ4959 and λ5007 lines, which make different contributions to the emission in B and V.

A periodicity and two trends, each on a time scale of 10–20 years, are clearly seen in the IR brightness variations of V1016 Cyg in 1978–2014.

We refined the pulsation period of the Mira, $P = 465 \pm 5$ days. The amplitude and scatter of the observed magnitudes in the periodic oscillations decrease with increasing wavelength, and the periodic IR brightness and color oscillations consist of separate cycles. The phase oscillations of the J and H magnitudes at minimum $J-H$ color index are about $1\fm4$. At the same time, the mean $J-H$ color index remains almost constant, and the periodic radial pulsations of the Mira can probably be responsible for the phase variations of the IR brightness and color.

In the case of long-term IR brightness variations (trends), the rise (decline) in IR brightness occurred with a simultaneous decrease (increase) in IR color indices. The dissipation of the envelope, into which both binary components were embedded before the outburst of the hot source in 1964, continued until the end of 1999; the optical depth of the dust envelope then began to increase, and this process has continued for the last ten years. The decline in brightness and reddening of the system in the near infrared reached their extreme values over the entire period of its observations by the end of 2014.

The distance to the Mira and its parameters were estimated from the observations of V1016 Cyg at maximum J brightness and at minimum $J-H$ color indices: $D = (2.95 \pm 0.16)$ kpc, $R_* = (470 \pm 50)\ R_\odot$, and $L_* = (9200 \pm 1900) L_\odot$.

We estimated the dust-envelope parameters for a simple model (the Mira heats a spherically symmetric and physically thin dust envelope). The dust-envelope temperature was taken to be 600 K, the dust grains in it were similar to dirty silicates, and their radius was 0.1 μm. Our analysis based on such a model showed that the bulk of the observed $J-K$ and $K-L$ color indices lie within the range of Mira temperatures from 2100 to 2700 K and optical depths from 0.5 to 2.5 at a wavelength of 1.25 μm, and the dust-envelope density, on average, decreased with increasing Mira temperature. The attenuation of the Mira emission by the dust envelope in 2014 reached almost 2^m in J and $4\fm5$ in V. Near its maximum and minimum IR brightness (in 2004 and 2012–2014), the Mira temperature was 2500 and 2400 K, the optical depths of the dust envelope (at $\lambda = 1.25$ μm) were 1 and 2.25, the dust-envelope radii were 10 600 $R_\odot$ and 9500 $R_\odot$, and the masses were $\sim 1.4 \times 10^{-6}$ M$_\odot$ and 2.5×10^{-6} $M_\odot$. The dust-envelope mass almost doubled in ten years, and the rate of dust supply into the dust envelope was $\sim 10^{-7}$ $M_\odot$ yr^{-1}.

The results of our spectrophotometry of the emission spectrum for the symbiotic nova 1016 Cyg in the range λ4300–7200 Å performed in 1995–2013 are as follows:

(1) The absolute fluxes in hydrogen, He I, He II, [Fe VII], [Ca VII], [O III], [Ar III], and [Ar V] lines showed a clear decrease in comparison with the preceding measurements of other authors by a factor of 1.3–3.0.

(2) The relative intensities of the forbidden [O III] λ4959 and λ5007 lines increased significantly after 2000, as did [Ar III] and [Ar V], although their absolute fluxes changed insignificantly over the period 1995–2013.

(3) The Raman O VI λ6825 line passed in its evolution through the maximum of its absolute intensity in 1995, having weakened almost by a factor of 10 by 2013 due to an increase in circumstellar extinction near the M component.

(4) Our estimate of the parameters of the gaseous envelope ejected by the hot star during its outburst showed that, in comparison with 1987, they changed very insignificantly. The electron density N_e was found from the hydrogen line fluxes to have decreased by less than a factor of 2. The electron density is high as before and close to 10^6 cm^{-3}, as is also indicated by the increase in the flux ratio of the nebular and auroral [O III] lines. The electron temperature in the [O III] emission zone is $\sim$20 000 K; it is $\sim$15 000 K in the [N II] (low) excitation zone at a density of $(1-2) \times 10^5$ cm^{-3}.

ACKNOWLEDGMENTS

This work was supported in part by the Russian Foundation for Basic Research (project no. 13-02-00136).

REFERENCES

1. F. J. Ahern, Astrophys. J. **197**, 639 (1975).
2. F. J. Ahern, Astrophys. J. **223**, 901 (1978).
3. V. P. Arkhipova, Perem. Zvezdy **22**, 25 (1983).
4. V. P. Arkhipova, V. F. Esipov, N. P. Ikonnikova, and G. V. Komissarova, Astron. Lett. **34**, 474 (2008).
5. M. S. Bessell, Publ. Astron. Soc. Pacif. **102**, 1181 (1990).
6. W. P. Blair, R. E. Stencel, W. A. Feibelman, and G. Michalitsianos, Astrophys. J. Suppl. Ser. **53**, 573 (1983).
7. M. Brocklehurst, Mon. Not. R. Astron. Soc. **153**, 471 (1971).
8. C. Brocksopp, M. F. Bode, S. P. S. Eyres, M. M. Crocker, R. Davis, and A. R. Taylor, Astrophys. J. **571**, 947 (2002).
9. M. A. Burlak, V. F. Esipov, G. V. Komissarova, V. I. Shenavrin, O. G. Taranova, A. M. Tatarnikov, and A. A. Tatarnikova, Baltic Astron. **24**, 109 2015.
10. E. R. Capriotti, Astrophys. J. **140**, 632 (1964).
11. F. Ciatti, A. Mammano, and A. Vittone, Astron. Astrophys. **68**, 251 (1978).
12. M. L. Clayton and M. W. Feast, Mon. Not. R. Astron. Soc. **146**, 411 (1969).
13. M. P. Fitzgerald and A. Pilavaki, Astrophys. J. Suppl. Ser. **28**, 147 (1974).
14. M. P. Fitzgerald, N. Houk, S. W. McCuskey, and D. Hoffleit, Astrophys. J. **144**, 1135 (1966).
15. I. S. Glass and M. W. Feast, Mon. Not. R. Astron. Soc. **198**, 199 (1982).
16. A. Gutiérrez-Moreno, H. Moreno, and G. Cortés, Publ. Astron. Soc. Pacif. **107**, 462 (1995).
17. K. H. Hinkle, F. C. Fekel, R. R. Joyce, and P. Wood, Astrophys. J. **770**, 28 (2013).
18. S. Hümmerich, S. Otero, P. Tisserand, and R. Bernhard, J. Am. Assoc. Var. Star. Observ. **43**, 1 (2015).
19. Y. Ikeda and S. Tamura, Publ. Astron. Soc. Jpn. **56**, 353 (2004).
20. A. P. Ipatov and B. T. Yudin, Astron. Astrophys. Suppl. Ser. **65**, 51 (1986).
21. R. J. Ivison, M. F. Bode, J. A. Roberts, J. Meaburn, R. J. Davis, R. F. Nelson, and R. E. Spencer, Mon. Not. R. Astron. Soc. **249**, 374 (1991).
22. H. L. Johnson, R. I. Mitchel, B. Iriarte, and W. Z. Wisniewski, Comm. Lunar Planet. Lab. **4**, 99 (1966).
23. T. W. Jones and K. M. Merrill, Astrophys. J. **209**, 509 (1976).
24. J. Koornneef, Astron. Astrophys. **128**, 84 (1983).
25. S. Kwok and D. A. Leahy, Astrophys. J. **283**, 675 (1984).
26. P. Lenz and M. Breger, Comm. Asteroseismol. **146**, 53 (2005).
27. V. M. Lyutyi, Soobshch. GAISh **172**, 30 (1971).
28. A. Mammano and F. Ciatti, Astron. Astrophys. **39**, 405 (1975).
29. E. M. McCade, Mon. Not. R. Astron. Soc. **200**, 71 (1982).
30. S. W. McCuskey, IAU Circ., No. 1916 (1965).
31. C. Mendoza, in *Proceedings of the IAU Symposium No. 103,* Ed. by D. R. Flower (Reidel, Dordrecht, Boston, London, 1983), p. 143.
32. U. Munari, Astron. Astrophys. **200**, L13 (1988).
33. U. Munari, B. F. Yudin, O. G. Taranova, G. Massone, et al., Astron. Astrophys. Suppl. Ser. **93**, 383 (1992).
34. U. Mürset and H. Nussbaumer, Astron. Astrophys. **282**, 586 (1994).
35. U. Mürset, W. Burkhard, and S. Jordan, Astron. Astrophys. **319**, 201 (1997).
36. H. Nussbaumer and H. M. Schmid, Astron. Astrophys. **101**, 118 (1988).
37. C. R. O'Dell, Astrophys. J. **149**, 373 (1967).
38. N. Oliversen and C. Anderson, Astrophys. J. **268**, 250 (1983).
39. S. Parimucha, V. Arkhipova, D. Chochol, et al., Contrib. Astron. Obs. Scalnate Pleso **30**, 93 (2000).
40. S. Parimucha, D. Chochol, T. Pribulla, L. M. Buson, and A. A. Vittone, Astron. Astrophys. **391**, 999 (2002).
41. B. S. C. Robertson and M. W. Feast, Mon. Not. R. Astron. Soc. **196**, 111 (1981).
42. R. J. Rudy, R. D. Cohen, G. S. Rossano, and R. C. Puetter, Astrophys. J. **362**, 346 (1990).

43. D. J. Schlegel, D. P. Finkbeiner, and M. Davis, Astrophys. J. **500**, 525 (1998).
44. H. M. Schmid and H. Schild, Mon. Not. R. Astron. Soc. **246**, 84 (1990).
45. H. M. Schmid and H. Schild, Astron. Astrophys. **395**, 117 (2002).
46. M. J. Seaton, Mon. Not. R. Astron. Soc. **187**, 73P (1979).
47. S. G. Sergeev and F. Heisberger, *A Users Manual for SPE* (Wien, 1993).
48. R. A. Shaw and R. J. Dufour, Publ. Astron. Soc. Pacif. **107**, 896 (1995).
49. V. I. Shenavrin, O. G. Taranova, and A. E. Nadzhip, Astron. Rep. **55**, 31 (2011).
50. H. Shild and H. M. Schmid, Astron. Astrophys. **310**, 211 (1996).
51. A. Skopal, New Astron. **12**, 597 (2007).
52. J. Solf, Astrophys. J. **266**, L113 (1983).
53. M. Sperl, Comm. Asteroseismol. **111**, 1 (1998).
54. O. G. Taranova, Astron. Lett. **34**, 404 (2000).
55. O. G. Taranova and B. F. Yudin, Astron. Astrophys. **117**, 209 (1983).
56. O. G. Taranova and V. I. Shenavrin, Astron. Lett. **26**, 600 (2000).
57. O. G. Taranova and B. F. Yudin, Sov. Astron. **30**, 193 (1986).
58. I. B. Voloshina et al., *Spectrophotometry of Bright Stars* (Nauka, Moscow, 1982) [in Russian].
59. G. Wallerstein, Astron. Astrophys. **197**, 161 (1988).
60. P. A. Whitelock, Publ. Astron. Soc. Pacif. **99**, 573 (1987).
61. P. A. Whitelock, M. W. Feast, and F. Leeuwen, Mon. Not. R. Astron. Soc. **386**, 313 (2008).
62. P. A. Whitelock, *AGB Stars and Related Phenomena, Proceedings of the Conference in Honor of Yoshikazu Nakada, National Astronomical Observatory of Japan, Mitaka, Tokyo, Japan, November 12–14, 2008,* Ed. by T. Ueta, N. Matsunaga, and Y. Ita (2009), p. 44.

Translated by V. Astakhov